Geophys. J. Int. (1990) **101**, 739–750 *and microfiche* GJI 101/1

Wave propagation in anisotropic linear viscoelastic media: theory and simulated wavefields

J. M. Carcione

Geophysical Institute, Hamburg University, Bundesstrasse 55, 2000 *Hamburg* 13, *FRG, and Osservatorio Geofisico Sperimentale, PO Box* 2011, 34016 *Trieste, Italy*

Accepted 1990 January 11. Received 1990 January 11; in original form 1988 October 10

SUMMARY

The anisotropic linear viscoelastic rheological relation constitutes a suitable model for describing the variety of phenomena which occur in seismic wavefields. This rheology, known also as Boltzmann's superposition principle, expresses the stress as a time convolution of a fourth rank tensorial relaxation function with the strain tensor.

The first problem is to establish the time dependence of the relaxation tensor in a general and consistent way. Two kernels based on the general standard linear solid are identified with the mean stress and with the deviatoric components of the stress tensor in a given coordinate system, respectively. Additional conditions are that in the elastic limit the relaxation matrix must give the elasticity matrix, and in the isotropic limit the relaxation matrix must approach the isotropic–viscoelastic matrix. The resulting rheological relation provides the framework for incorporating anelasticity in time-marching methods for computing synthetic seismograms. Through a plane wave analysis of the anisotropic–viscoelastic medium, the phase, group and energy velocities are calculated in function of the complex velocity, showing that those velocities are in general different from each other. For instance, the energy velocity which represents the wave surface, is different from the group velocity unlike in the anisotropic–elastic case. The group velocity loses its physical meaning at the cusps where singularities appear. Each frequency component of the wavefield has a different non-spherical wavefront. Moreover, the quality factors for the different propagating modes are not isotropic. Examples of these physical quantities are shown for transversely isotropic–viscoelastic clayshale and sandstone.

As in the isotropic–viscoelastic case, Boltzmann's superposition principle is implemented in the equation of motion by defining memory variables which circumvent the convolutional relation between stress and strain. The numerical problem is solved by using a new time integration technique specially designed to deal with wave propagation in linear viscoelastic media. As a first application snapshots and synthetic seismograms are computed for 2-D transversely isotropic–viscoelastic clayshale and sandstone which show substantial differences in amplitude, waveform and arrival time with the results given by the isotropic and elastic rheologies.

Key words: anisotropy, attenuation, dispersion, modelling, viscoelasticity.

INTRODUCTION

The following abbreviations are used for simplicity: IE: isotropic–elastic, IV: isotropic–viscoelastic, TIE: transversely isotropic–elastic, AE: anisotropic–elastic, TIV: transversely isotropic–viscoelastic, and AV: anisotropic–viscoelastic.

With the improvement in data quality and the use of new exploration techniques, the correct description of the seismic wavefield has become more important. This task has become feasible with the development of new algorithms for solving the governing equation of motion, and the availability of better computational facilities. An appropriate theory for describing wave propagation in the Earth should

Downloaded from https://academic.oup.com/gji/article/101/3/739/602971 by guest on 21 August 2022

include all the phenomena which can be detected and measured in real seismic data. Of importance to earthquake seismologists and exploration geophysicists is the following approximate chronological order for the introduction of the different rheologies in seismic modelling.

(a) A first approximation to model the compressional wavefield or *P*-wave by assuming the acoustic rheology. In general, the commercial processing software for petroleum geophysics is based on this approximation.

(b) The IE rheology to replace the acoustic assumption (see for instance Alekseev & Mikhailenko, 1980; Kosloff, Reshef & Loewenthal 1984; Virieux 1986; Kummer, Behle & Dorau 1987), which gives the distinction between the compressional and the shear wavefields, and the conversion from one mode to the other.

(c) The incorporation of attenuation into the acoustic rheology, giving the viscoacoustic stress–strain relation (Krebes & Hron 1980; Day & Minster 1984; Emmerich & Korn 1987; Carcione, Kosloff & Kosloff 1988a, b). This rheology explains the attenuation and dispersion of the dilatational wavefield.

(d) The IV rheology (see for instance Mikhailenko 1985; Carcione *et al.* 1988c), which in many aspects describes new effects compared to the purely elastic case (Buchen 1971; Borcherdt & Wennerberg 1985); for instance, the existence of inhomogeneous waves (not the interface waves of elastic media) makes it necessary to satisfy the boundary conditions on anelastic interfaces. For these waves the propagation direction does not coincide with the attenuation direction, particle motions are elliptical, and critical angles do not exist in general but only under particular circumstances. In general, a wave travelling through a layered media has an angular dependence of attenuation and dispersion, where the more oblique direction has more energy dissipation and lower velocity.

(e) The AE rheology (see for instance White 1982; Booth & Crampin 1983; Martynov & Mikhailenko 1984; Fryer & Frazer 1987; Gajewski & Pšenčík 1988; Carcione *et al.* 1988d), which introduces new phenomena, for instance shear wave splitting (Crampin 1985). The most important consequences of this rheology are that in general, the wavefield is not pure longitudinal or pure transverse, and therefore there is no simple relation between the propagation direction and the direction of particle displacement; wavefronts are not spherical; the direction of energy flux (rays) does not coincide with the wavenumber direction. A secondary effect, not detected yet in seismic data, are the cusps present in one of the shear modes.

A further and natural step for obtaining a realistic description, i.e., the inclusion in wave propagation of all the phenomena mentioned before, is the implementation of the linear AV constitutive relation in the equation of motion. The linear assumption for the dissipation mechanisms is justified by experimental results found for seismic strains and upper crustal conditions (Jones 1986). Anelasticity is due to a rather large number of physical mechanisms depending on the frequency band (Biot 1962; O'Connell & Budiansky 1977; Murphy, Winkler & Kleinberg 1986; etc.). A general way to account for all these mechanisms is to use a phenomenological model which can fit any particular theory and also real data. On the other hand, anisotropy is well described by the generalized Hooke's law, i.e., by 21 independent elastic constants in a 3-D medium, and six elastic constants in a 2-D medium.

The most general rheology under these circumstances is the isothermal AV constitutive relation (Christensen 1982), in which the stress and the strain tensors are related by a time-dependent relaxation tensor through a convolution integral. The first problem is to establish the time dependence of the relaxation tensor in a general and consistent way. The kernel represented by the general standard linear solid is the basis for constructing this time dependence. A general viscoelastic solid can be obtained by considering several standard linear elements in parallel or in series. It is important, particularly in exploration seismology, that the material rheology gives causal behaviour and approximately a constant Q factor in the exploration seismic band, although the kernel can fit any general Q function no matter what the frequency range. The process of wave propagation in porous media can be approximated by a linear viscoelastic solid when wave propagating modes are considered. It was showed by Geertsma & Smit (1961) that to describe *P*-wave propagation in a Biot medium one standard linear element is sufficient.

Two kernels or relaxation functions are identified, one of them with the mean stress which is invariant under transformations of the coordinate system, and the other with the deviatoric components of the stress tensor in a given coordinate system. In this way it is possible to establish the anelastic characteristics of the three propagating modes, the quasi-longitudinal and the two shear modes. Two additional conditions are imposed: (i) in the AE limit the relaxation matrix must approach the elasticity matrix, and (ii) in the IV limit the relaxation matrix must give the isotropic–viscoelastic matrix defined in Carcione *et al.* (1988c). The resulting constitutive relation, although not unique, represents a general and consistent way to introduce anelasticity into the generalized Hooke's law. The preceding conditions establish the time dependence of the relaxation matrix components on physical grounds, and maintain the simplicity of the isotropic case where only two kernels are necessary to define the anelastic properties. As in the IV wave propagation problem, Boltzmann's superposition principle is implemented in the equation of motion by defining memory variables which circumvent the convolutional relation between stress and strain. For instance, the solution of the 2-D problem implies the introduction of three memory variables, one for each dilatational relaxation mechanism and two for each shear relaxation mechanism.

This work concentrates on the issue of wave propagation in the Earth. However, the subject of wave propagation in AV media has practical a value in many other fields, for instance applied mechanics and physics of materials (see for instance Lamb & Richter 1966; Szilard 1982). The first section establishes the constitutive relation. Then, the equation of motion for a general inhomogeneous AV medium is derived. Finally, examples of wave propagation in 2-D homogeneous and inhomogeneous TIV real earth materials are considered, with comparisons to the more simple rheologies. The microfiche contains the following material: first a detailed derivation of the constitutive relation; then a plane wave analysis establishes the energy balance equation and the phase, group and energy velocities

Downloaded from https://academic.oup.com/gji/article/101/3/739/602971 by guest on 21 August 2022

of the AV medium, with 3-D examples for TIV earth media; finally, the derivation of the equation of motion for 2-D TIV media with simulated wavefields in sandstone.

CONSTITUTIVE RELATION

The stress–strain relation is simplified by introducing a shortened matrix notation where pairs of subscripts are replaced by a single number according to the following correspondences: $(11)\to 1$, $(22)\to 2$, $(33)\to 3$, $(23)=(32)\to 4$, $(13)=(31)\to 5$, $(12)=(21)\to 6$. The convention will be to denote abbreviated subscripts by upper case letters and full subscripts by lower case letters.

A response of the earth is described by Boltzmann's superposition principle which can be expressed as (see Appendix A in microfiche):

$$\mathbf{T}(\mathbf{x}, t) = \Psi(\mathbf{x}, t) * \mathbf{S}(\mathbf{x}, t), \tag{1}$$

with

$$\mathbf{T}^{\mathrm{T}} = (T_1, T_2, T_3, T_4, T_5, T_6) = (\sigma_{xx}, \sigma_{yy}, \sigma_{zz}, \sigma_{yz}, \sigma_{xz}, \sigma_{xy}) \tag{2}$$

the stress vector, where σ_{ij}, $i, j = 1, \ldots, 3$ are the stress components, and

$$\mathbf{S}^{\mathrm{T}} = (S_1, S_2, S_3, S_4, S_5, S_6) = (\varepsilon_{xx}, \varepsilon_{yy}, \varepsilon_{zz}, 2\varepsilon_{yz}, 2\varepsilon_{xz}, 2\varepsilon_{xy}) \tag{3}$$

the strain vector, where ε_{ij}, $i, j = 1, \ldots, 3$ are the strain components; Ψ is the symmetric relaxation matrix with components ψ_{IJ}, $I, J = 1, \ldots, 6$; t is the time variable, $\mathbf{x}$ is the position vector, the symbol '*' indicates time convolution, and a dot above a variable implies time differentiation. Vectors are written as columns with the superscript 'T' denoting the transpose.

Equation (1) can be written in components as

$$T_I = \psi_{IJ} * \dot{S}_J, \qquad I, J = 1, \ldots, 6 \tag{4}$$

where the Einstein convention for repeated indices is used. In Appendix A, the following stress–strain relation is established:

$$T_I = \psi_{IJ} * \dot{S}_J = \{[A_{IJ} + A_{IJ}^{(\nu)}\chi_\nu(t)]H(t)\} * \dot{S}_J, \tag{5}$$

where χ_ν, $\nu = 1, 2$ are time-dependent functions, and A_{IJ} and $A_{IJ}^{(\nu)}$ are space-dependent functions. The conditions on the relaxation components are that the trace of the stress tensor should depend on the time variable only through the kernel χ_1, and the deviatoric components of the stress tensor in a given system S should depend on the time variable only through the kernel χ_2. The trace of the stress tensor is invariant under transformation of the coordinate system. This fact assures that the mean tension (one third of the trace) is related only to the function χ_1 in any system. Hence, this function describes dilatational deformations. The deviatoric components are not invariants but a cube of material orientated in the direction of the axes of the system S will be subjected to shear deformations exclusively related to the function χ_2. In general, experimental values of the attenuation coefficient and the quality factor are given with respect to material axes (Lamb & Richter 1966). With this condition for instance, the value of the shear quality factors in the symmetry axis of a TIV medium can be established. Additional conditions are that in the AE limit the relaxation matrix must give the elasticity matrix, and that in the IV limit the relaxation matrix must give the isotropic–viscoelastic matrix (Carcione *et al.* 1988c). In Appendix A an appropiate 3-D AV relaxation matrix is obtained which has the form

$$\Psi = \begin{pmatrix} \psi_{11}\psi_{12}\psi_{13} & c_{14} & c_{15} & c_{16} \\ \psi_{22}\psi_{23} & c_{24} & c_{25} & c_{26} \\ \psi_{33} & c_{34} & c_{35} & c_{36} \\ & c_{44}\chi_2 & c_{45}\chi_2 & c_{46}\chi_2 \\ & & c_{55}\chi_2 & c_{56}\chi_2 \\ & & & c_{66}\chi_2 \end{pmatrix} H \tag{6}$$

with

$$\psi_{11} = c_{11} - D + (D - \tfrac{4}{3}G)\chi_1 + \tfrac{4}{3}G\chi_2, \tag{7a}$$

$$\psi_{12} = c_{12} - D + 2G + (D - \tfrac{4}{3}G)\chi_1 - \tfrac{2}{3}G\chi_2, \tag{7b}$$

$$\psi_{13} = c_{13} - D + 2G + (D - \tfrac{4}{3}G)\chi_1 - \tfrac{2}{3}G\chi_2, \tag{7c}$$

$$\psi_{22} = c_{22} - D + (D - \tfrac{4}{3}G)\chi_1 + \tfrac{4}{3}G\chi_2, \tag{7d}$$

$$\psi_{23} = c_{23} - D + 2G + (D - \tfrac{4}{3}G)\chi_1 - \tfrac{2}{3}G\chi_2, \tag{7e}$$

and

$$\psi_{33} = c_{33} - D + (D - \tfrac{4}{3}G)\chi_1 + \tfrac{4}{3}G\chi_2, \tag{7f}$$

where $H(t)$ is the Heaviside function,

$$D = (c_{11} + c_{22} + c_{33})/3 \tag{7g}$$

and

$$G = (c_{44} + c_{55} + c_{66})/3. \tag{7h}$$

The quantities c_{IJ}, $I, J = 1, 6$ represent space-dependent elasticities, and

$$\chi_\nu = \left[1 - \sum_{l=1}^{L_\nu}\left(1 - \frac{\tau_{el}^{(\nu)}}{\tau_{ol}^{(\nu)}}\right)\mathrm{e}^{-t/\tau_{ol}^{(\nu)}}\right], \qquad \nu = 1, 2 \tag{8}$$

are relaxation functions which correspond to states of quasi-dilatation ($\nu = 1$), and quasi-shear ($\nu = 2$), respectively. The quantities $\tau_{el}^{(\nu)}(\mathbf{x})$ and $\tau_{ol}^{(\nu)}(\mathbf{x})$ denote material relaxation times for lth mechanism, and L_ν is the number of relaxation mechanisms. Although the kernels χ_ν are based on the standard linear solid any appropriate kernel can also be used, for instance the generalized Maxwell body given by Emmerich & Korn (1987).

An example of a 2-D relaxation matrix is

$$\Psi = \begin{pmatrix} \psi_{11}\psi_{12} & c_{15} \\ \psi_{22} & c_{35} \\ & c_{55}\chi_2 \end{pmatrix} H, \tag{9}$$

with

$$\psi_{11} = c_{11} - D + (D - c_{55})\chi_1 + c_{55}\chi_2, \tag{10a}$$

$$\psi_{12} = c_{13} + 2c_{55} - D + (D - c_{55})\chi_1 - c_{55}\chi_2, \tag{10b}$$

$$\psi_{22} = c_{33} - D + (D - c_{55})\chi_1 + c_{55}\chi_2, \tag{10c}$$

and

$$D = (c_{11} + c_{33})/2, \tag{10d}$$

Downloaded from https://academic.oup.com/gji/article/101/3/739/602971 by guest on 21 August 2022

where the (x, z)-plane has been considered. The elastic limit is obtained when $\chi_\nu \to 1$, $\nu = 1, 2$, which can be verified easily in equations (6) and (9).

Uniform plane waves provide a very useful tool for analysing characteristics of wave propagation. In Appendix B (microfiche) a plane wave analysis of an AV medium is performed. First the energy balance equation or complex Poynting's theorem is established. Then, the Christoffel equation and dispersion relation. Finally, the complex and physical velocities of the three modes are obtained together with the quality factors for homogeneous waves. Physical velocities mean the phase velocity or wavefront velocity along the propagation direction, the group velocity or velocity of the modulation envelope of the wave, and the energy velocity which has the direction of the Poynting vector, and its representation defines the wave surface. As a consequence, the relations among the different physical velocities and quality factors for the various rheologies are summarized. The examples show the wave propagation characteristics of a TIV clayshale and a TIV sandstone. The Appendix contains also a verification of the physical realizability conditions of the relaxation matrix.

EQUATION OF MOTION

The equation of motion for a 3-D anisotropic linear anelastic medium is

$$\nabla \cdot \mathbf{T} = \rho \ddot{\mathbf{u}} + \mathbf{f}, \tag{11}$$

or in components

$$\nabla_{iJ} T_J = \rho \ddot{u}_i + f_i, \tag{12}$$

where $\mathbf{u}(\mathbf{x}, t)$ is the displacement vector, $\mathbf{f}(\mathbf{x}, t)$ is the body forces vector, $\rho(\mathbf{x})$ is the density, and '$\nabla \cdot$' is a divergence operator defined by

$$\nabla \cdot \to \nabla_{iJ} = \begin{pmatrix} \partial/\partial x & 0 & 0 & 0 & \partial/\partial z & \partial/\partial y \\ 0 & \partial/\partial y & 0 & \partial/\partial z & 0 & \partial/\partial x \\ 0 & 0 & \partial/\partial z & \partial/\partial y & \partial/\partial x & 0 \end{pmatrix}. \tag{13}$$

As in the IV wave propagation problem (Carcione *et al.* 1988c), implementation of the rheological relation (5) is not straightforward because of the presence of convolutional kernels. Consequently, in this section the constitutive equation is reformulated to yield a more convenient description. Let the relaxation matrix be known in system S', and the problem solved in system S. Therefore, the relaxation components transform as

$$\psi_{IJ} = t_{IL} t_{JK} \psi'_{LK}, \tag{14}$$

where $\boldsymbol{\Psi}'$ is the relaxation matrix in system S', and $\mathbf{T}$ is a 6×6 rotation with components t_{IJ} (see Appendix C in microfiche). These components can be space dependent. Combining equations (5) and (14) and using properties of the convolution gives

$$T_I = t_{IL} t_{JK} \left[A_{LK} S_J + A_{LK}^{(\nu)} \frac{d}{dt} (\chi_\nu H) * S_J \right] \tag{15}$$

where the primes in the relaxation components are omitted for clarity. Equation (15) is equivalent to

$$T_I = t_{IL} t_{JK} \{ [A_{LK} + A_{LK}^{(\nu)} \chi_\nu(0)] S_J + A_{LK}^{(\nu)} \dot{\chi}_\nu * S_J \}, \tag{16}$$

after the integration of the resulting delta function. Performing the time derivative [see equation (8)], yields

$$T_I = t_{IL} t_{JK} \left\{ [(A_{LK} + A_{LK}^{(\nu)} M_{u\nu}] S_J + A_{LK}^{(\nu)} \sum_{l=1}^{L_\nu} \varphi_{\nu l} * S_J \right\}, \tag{17}$$

where

$$\varphi_{\nu l} = \frac{1}{\tau_{\sigma l}^{(\nu)}} \left(1 - \frac{\tau_{\varepsilon l}^{(\nu)}}{\tau_{\sigma l}^{(\nu)}} \right) e^{-t/\tau_{\sigma l}^{(\nu)}}, \qquad l = l, \ldots, L_\nu \tag{18}$$

is called the response function of the lth relaxation mechanism, and $M_{u\nu} \equiv \chi_\nu(0)$ is the unrelaxed modulus. The function $\varphi_{\nu l}$ obeys the following differential equation:

$$\dot{\varphi}_{\nu l}(t) = -\varphi_{\nu l}(t)/\tau_{\sigma l}^{(\nu)}. \tag{19}$$

Now the following memory variables are defined:

$$e_{Jl}^{(\nu)} = \varphi_{\nu l} * S_J, \ \nu = 1, 2, \ J = 1, \ldots, 6, \ l = 1, \ldots, L_\nu. \tag{20}$$

Replacing these quantities in (17) yields

$$T_I = t_{IL} t_{JK} \left\{ [A_{LK} + A_{LK}^{(\nu)} M_{u\nu}] S_J + A_{LK}^{(\nu)} \sum_{l=1}^{L_\nu} e_{JL}^{(\nu)} \right\}. \tag{21}$$

Time defferentiating equation (20) gives

$$\dot{e}_{Jl}^{(\nu)} = S_J \varphi_{\nu l}(0) - e_{Jl}^{(\nu)}/\tau_{\sigma l}^{(\nu)}, \qquad l = 1, \ldots, L_\nu, \tag{22}$$

where equation (19) has been used. Equation (21) and (22) together with the equation of motion (12) fully describe the response of the AV medium, and will be the basis for the numerical solution algorithm. After substitution of (21) in (12), and with equations (22) and the strain–displacement relations, a first-order differential equation in time is obtained:

$$\dot{\mathbf{U}} = \mathbf{M}\mathbf{U} + \mathbf{F}, \tag{23}$$

where $\mathbf{U}$ is the unknown variable vector formally given by

$$\mathbf{U}^{\mathrm{T}} = (\mathbf{u}, \dot{\mathbf{u}}, e_{Jl}^{(\nu)}), \tag{24}$$

$\mathbf{F}$ is the body force vector represented by

$$\mathbf{F}^{\mathrm{T}} = (\mathbf{0}, \mathbf{f}/\rho, \mathbf{0}), \tag{25}$$

and $\mathbf{M}$ is an operator matrix which contains the spatial derivative operators and all the material parameters defining the medium. In the next section this operator is given explicitly for the 2-D case. The number of memory variables depends on the particular choice of the relaxation matrix, but in principle they are reduced in virtue of the restrictions imposed on the relaxation components. The rotation type also restricts the number of variables. It can be seen that when $\mathbf{T}$ is the identity matrix, the number of variables reduce to a minimum. An alternative method to equation (14) is to apply the transformation to the elasticity matrix $\mathbf{C}$ (whose components are c_{IJ}, $I, J = 1, \ldots, 6$) and then introduce the anelasticity. Of course these two different approaches do not give the same results, but the latter case requires a minimum of variables. In the next section an example of 2-D wave propagation is considered, where the

Downloaded from https://academic.oup.com/gji/article/101/3/739/602971 by guest on 21 August 2022

problem can be treated with three variables for each relaxation mechanism.

The differential equation (23) represents the equation of motion for the AV medium which correctly describes anisotropic and anelastic effects in wave propagation within the framework of the linear response theory.

The solution of (23) subject to the initial condition $\mathbf{U}(t=0)=\mathbf{U}_0$ is formally given by

$$\mathbf{U}=e^{t\mathbf{M}}\mathbf{U}_0+\int_0^t e^{\tau\mathbf{M}}\mathbf{F}(t-\tau)\,d\tau. \tag{26}$$

In equation (26), $e^{t\mathbf{M}}$ is called the evolution operator of the system. Most frequently an explicit or implicit finite difference scheme is used to march the solution in time in the AE and IV wave propagation problems. This technique is based on a Taylor expansion of the evolution operator. This work uses a new time integration method which is specially designed to deal with wave propagation in linear AV media. The new approach is based on a polynomial interpolation of the exponential function in the complex domain of the eigenvalues of the operator $\mathbf{M}$, in a set of points which is known to have some maximal properties. In this way, the interpolating polynomial is 'almost best'. The spatial derivative terms are computed by means of the Fourier method (Kosloff & Baysal 1982). The advantages of this new algorithm over finite differencing in time can be found in Tal-Ezer, Carcione & Kosloff (1989).

2-D WAVE PROPAGATION

For simplicity a 2-D TIV medium with symmetry axis parallel to the z-axis is considered. Then, the rotation matrix $\mathbf{T}$ is the identity matrix. The rheological relation is given by equation (9), with $c_{15}=c_{35}=0$. Choosing one relaxation mechanism for each mode ($L_1=L_2=1$) the unknown variable vector is given by (see Appendix D in microfiche),

$$\mathbf{U}^{\mathrm{T}}=(u_x,\,u_z,\,\dot{u}_x,\,\dot{u}_z,\,e_1,\,e_2,\,e_3), \tag{27}$$

where $e_1=e_{11}^{(1)}+e_{31}^{(1)}$, $e_2=e_{11}^{(2)}-e_{31}^{(2)}$, and $e_3=e_{51}^{(2)}$ in terms of the memory variables (20). The body forces vector is

$$\mathbf{F}^{\mathrm{T}}=(0,0,f_x/\rho,f_z/\rho,0,0,0), \tag{28}$$

and the spatial operator

$$\mathbf{M}=\begin{pmatrix} 0 & 0 & 1 & 0 & 0 & 0 & 0\\ 0 & 0 & 0 & 1 & 0 & 0 & 0\\ M_{31} & M_{32} & 0 & 0 & M_{35} & M_{36} & M_{37}\\ M_{41} & M_{42} & 0 & 0 & M_{45} & M_{46} & M_{47}\\ M_{51} & M_{52} & 0 & 0 & M_{55} & 0 & 0\\ M_{61} & M_{62} & 0 & 0 & 0 & M_{66} & 0\\ M_{71} & M_{72} & 0 & 0 & 0 & 0 & M_{77} \end{pmatrix}, \tag{29}$$

with

$$\rho M_{31}=\partial/\partial x[(c_{11}-D)+(D-c_{55})M_{u1}+c_{55}M_{u2}]\,\partial/\partial x+\partial/\partial z(c_{55}M_{u2})\,\partial/\partial z, \tag{30a}$$

$$\rho M_{32}=\partial/\partial x[(c_{13}+2c_{55}-D)+(D-c_{55})M_{u1}-c_{55}M_{u2}]\times\partial/\partial z+\partial/\partial z(c_{55}M_{u2})\,\partial/\partial x, \tag{30b}$$

$$\rho M_{35}=\partial/\partial x(D-c_{55}),\quad \rho M_{36}=\partial/\partial x c_{55},\quad \rho M_{37}=\partial/\partial z c_{55}, \tag{30c}$$

$$\rho M_{41}=\partial/\partial z[(c_{13}+2c_{55}-D)+(D-c_{55})M_{u1}-c_{55}M_{u2}]\times\partial/\partial z+\partial/\partial x(c_{55}M_{u2})\,\partial/\partial z, \tag{30d}$$

$$\rho M_{42}=\partial/\partial z[(c_{33}-D)+(D-c_{55})M_{u1}+c_{55}M_{u2}]\,\partial/\partial z+\partial/\partial x(c_{55}M_{u2})\,\partial/\partial x, \tag{30e}$$

$$\rho M_{45}=\partial/\partial z(D-c_{55}),\quad \rho M_{46}=-\partial/\partial z c_{55},\quad \rho M_{47}=\partial/\partial x c_{55}, \tag{30f}$$

$$M_{51}=\varphi_1(0)\,\partial/\partial x,\quad M_{52}=\varphi_1(0)\,\partial/\partial z,\quad M_{55}=-1/\tau_\sigma^{(1)}, \tag{30g}$$

$$M_{61}=\varphi_2(0)\,\partial/\partial x,\quad M_{62}=\varphi_2(0)\,\partial/\partial z,\quad M_{66}=-1/\tau_\sigma^{(2)}, \tag{30h}$$

and

$$M_{71}=\varphi_2(0)\,\partial/\partial z,\quad M_{72}=\varphi_2(0)\,\partial/\partial x,\quad M_{77}=-1/\tau_\sigma^{(2)}, \tag{30i}$$

where the sub-index l denoting a physical mechanism has been omitted for simplicity. For a general number of physical mechanisms the number of memory variables is given by $n_v=L_1+2L_2$. The examples presented in the next section, for instance, use $L_1=L_2=2$; therefore $n_v=6$. The spatial operator for an elastic solid is obtained by taking the limit $M_{uv}\to 1$, $\varphi_v(0)\to 0$, $v=1,2$.

EXAMPLES

The first example involves wave propagation in 2-D homogeneous TIV media, a clayshale and a sandstone whose material properties are given in Table 1. The relaxation times give almost constant Q in the exploration seismic band. Similar materials with moderate to large amounts of absorption were reported by Mc Donal *et al.* (1958) for Pierre shale ($Q_{\mathrm{P}}=10$), and ocean bottom sediments by Hamilton *et al.* (1970), with Q_{P} ranging from 1 to 5. Isotropic versions are obtained by choosing the isotropic compressional and shear wave velocities as the pure longitudinal and pure transverse velocities (vertical direction) of the anisotropic material. The elasticities for the isotropic media are given in Table 1.

This section shows results for homogeneous clayshale and Appendix E (see microfiche) for homogeneous sandstone.

Table 1. Material properties of the TIV media.

Medium	Elasticities and density						
	c_{11} (GPa)	c_{12} (GPa)	c_{13} (GPa)	c_{33} (GPa)	c_{55} (GPa)	c_{66} (GPa)	ρ (Kg/m^3)
ANI Clayshale	66.6	19.7	39.4	39.9	10.9	23.4	2590.
ANI Sandstone	80.2	25.2	−5.0	80.2	27.9	27.5	2690.
ISO Clayshale	39.9	18.1	18.1	39.9	10.9	10.9	2590.
ISO Sandstone	80.2	24.4	24.4	80.2	27.9	27.9	2690.

	Relaxation times				
	l	$\tau_{\varepsilon l}^{(1)}$ (s)	$\tau_{\sigma l}^{(1)}$ (s)	$\tau_{\varepsilon l}^{(2)}$ (s)	$\tau_{\sigma l}^{(2)}$ (s)
Clayshale	1	0.0332577	0.0304655	0.0352443	0.0287482
	2	0.0033257	0.0030465	0.0029370	0.0023957
Sandstone	1	0.0325305	0.0311465	0.0332577	0.0304655
	2	0.0032530	0.0031146	0.0033257	0.0030465

Downloaded from https://academic.oup.com/gji/article/101/3/739/602971 by guest on 21 August 2022

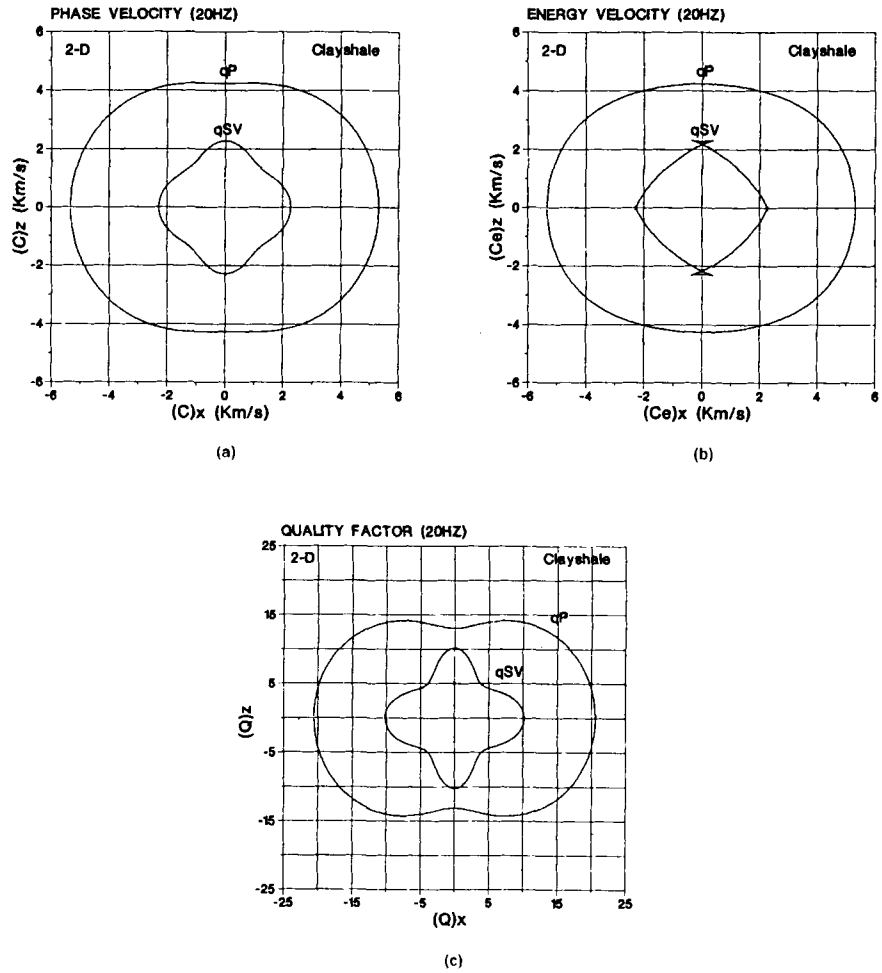

Figure 1. 2-D TIV clayshale, (a) phase velocity, (b) energy velocity curves (wavefronts), (c) quality factor curves. Frequency is 20 Hz. At the low- and high-frequency limits the energy velocities present minimum and maximum values respectively, while the quality factors are infinity. More details can be found in Appendix B (microfiche).

Fig. 1 displays polar representations of (a) phase velocity, (b) energy velocity, and (c) quality factors, at a frequency of $f = 20$ Hz. The expressions for these quantities are given in Appendix B with a complete analysis of the 3-D case for the same materials. The energy velocity curves present sections of the wavefront. As can be seen in Figs 1(a) and (c) the quality factor curves follow approximately the shape of the phase velocity curves.

The modelling uses a 165×165 grid mesh with $DX = DZ = 20$ m grid spacing. The motion is initiated by a vertical impulsive force located in the centre of the homogeneous region. The time function is given by

$$h(t) = e^{1/2 f_0^2 (t - t_0)^2} \cos [\pi f_0 (t - t_0)], \tag{31}$$

where $t_0 = 0.06$ s, and $f_0 = 50$ Hz is the cut-off frequency. This wavelet resembles a vibrator signal after the autocorrelation.

Figures 2 and 3 display the u_x and u_z components at $t = 0.32$ s for the different rheologies. The number between parenthesis denotes the plotting scale. The viscoelastic amplitudes are taken as references; scale 10 means that the amplitudes are reduced by a factor 10. All the wavefronts show the characteristics predicted by the theory. In the elastic case the shear wave amplitude is much stronger than the compressional wave amplitude, while in the anelastic case these amplitudes are comparable (except in the cusps) due to the higher attenuation acting on the shear mode. As predicted by the energy velocity curve, the anelastic wavefronts are greater than the elastic wavefronts, and the waveform appears broader due to the velocity dispersion. This dispersion effect is manifested also in the low amplitude tails following the qP- and qSV-wavefronts. The differences between the elastic and anelastic wavefronts have to be considered in relative terms. If the elastic limit is chosen in the high-frequency limit, the elastic wavefronts appear bigger than the anelastic wavefronts. A comparison between the AV and IE snapshots show important differences in amplitude, waveshape and arrival time. In some directions the anisotropic and anelastic effects compensate each other to give approximately the same arrival time in both cases (for instance at the angle $\theta = \pi/4$).

Since there is no analytical solution for the AV wave propagation problem, it is not possible, as with the other rheologies, to test the accuracy of the algorithm. As a reference, the AE u_z component in the symmetry axis is compared to analytical solution (see Carcione *et al.* 1988d). As Fig. 4 shows, the comparison is excellent. From Fig. 2 the u_x component along the symmetry axis is zero according

Downloaded from https://academic.oup.com/gji/article/101/3/739/602971 by guest on 21 August 2022

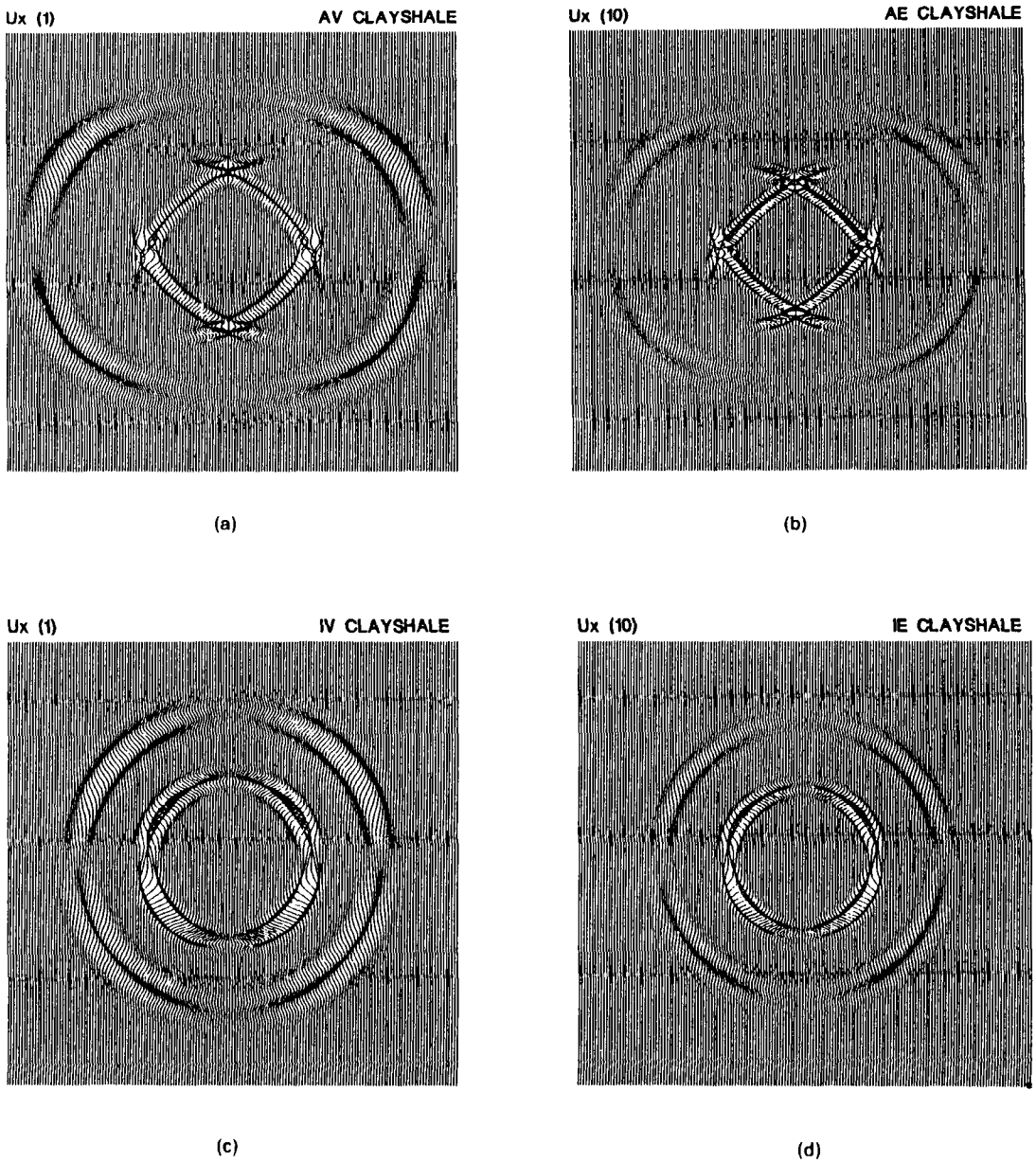

Figure 2. u_x component of the wavefield at $t = 0.32$ s for TIV clayshale, (a) AV rheology, (b) AE rheology, (c) IV rheology, (d) IE rheology. The motion is initiated by a vertical source. The number between parenthesis denotes the plotting scale. The elastic amplitudes are reduced by a factor 10 relative to the viscoelastic amplitudes.

to the analytical solution. The same accuracy in the AV case is expected.

Synthetic seismogram comparisons in the symmetry axis at distances of 100 and 200 m from the source are displayed in Figs 5 and 6 for the u_z component. At 100 m the anelastic effects produce a destructive interference between the qP and qSV modes, and the AV solution looks quite different compared to the other solutions. At 200 m the two modes start to separate and it is evident that the shear mode is relatively faster than the compressional mode. Although the symmetry axis is a pure mode direction, the differences in amplitude and waveform between the AV solution and the other solutions are important. Figs 7(a) and (b) display the comparison between the u_z component of AE and AV clayshale in the symmetry axis and at $\theta = \pi/4$ respectively. The stations are located at 400 m from the source in both cases. As indicated by the quality factor in Fig. 1, the qSV mode is more attenuated at $\theta = \pi/4$ than in the symmetry axis; while for the qP mode the opposite behaviour occurs. These effects can be appreciated in Fig. 7.

A final example illustrates wave propagation in an inhomogeneous medium. An interface separates two half-spaces; the upper medium is TIV sandstone with the symmetry axis making an angle $\beta = \pi/4$ with the vertical axis, and the lower medium is IE sandstone. The source is located on the interface and has the symmetry axis direction. To solve the problem the rotation has been applied to the elasticity matrix $\mathbf{C}$. As in the previous example the formulation requires three memory variables. Figs 8(a) and (b) display the u_x and u_z components at

Downloaded from https://academic.oup.com/gji/article/101/3/739/602971 by guest on 21 August 2022

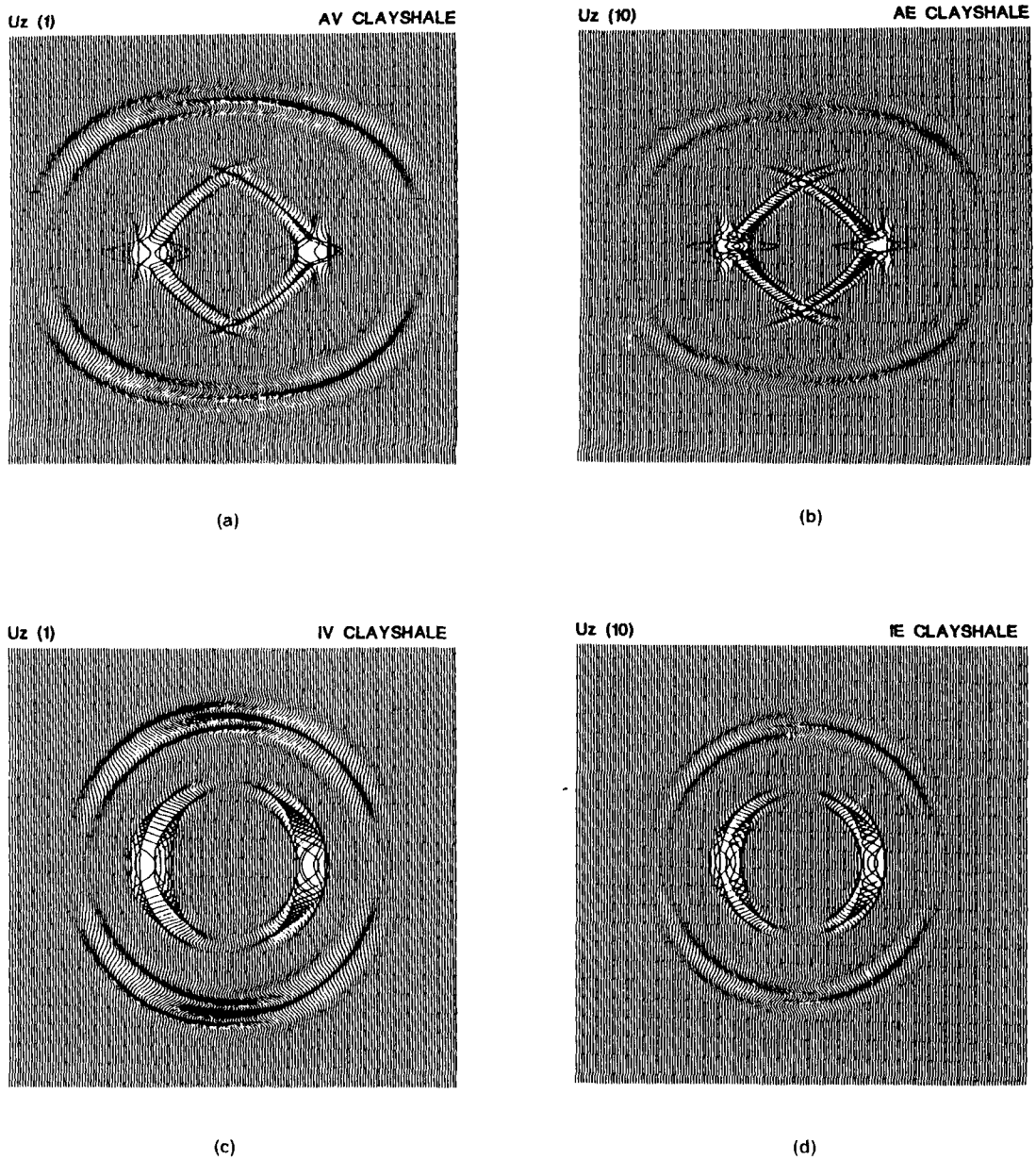

Figure 3. u_z component of the wavefield at $t = 0.32$ s for TIV clayshale, (a) AV rheology, (b) AE rheology, (c) IV rheology, (d) IE rheology. The motion is initiated by a vertical source. The number between parenthesis denotes the plotting scale. The elastic amplitudes are reduced by a factor 10 relative to the viscoelastic amplitudes.

$t = 0.32$ s. The diagonal line indicates the symmetry axis direction. The wave characteristics in the upper medium are similar to those when $\beta = 0$ (no rotation, see Appendix E). However, as mentioned before, in order to obtain the same solution the rotation should be applied to the relaxation matrix.

CONCLUSIONS

A general theory for describing wave propagation in anisotropic linear viscoelastic media requires the use of Boltzmann's superposition principle. Two kernels are sufficient to establish the anelastic characteristics of the wavefield; one of them is identified with the quasi-dilatational mode and the other with the quasi-shear modes. The resulting rheological relation provides the framework for computing numerical anisotropic–viscoelastic wavefields.

An analysis of a transversely isotropic–viscoelastic medium by considering homogeneous waves reveals the wave characteristics. Each frequency component has a different non-spherical wavefront. The energy and group velocities coincide only at the low- and high-frequency limits. Quality factors and velocity dispersion are not isotropic. As in the elastic anisotropic case the wavenumber vector is normal to the wavefront, and the energy velocity vector is normal the phase velocity surface.

Downloaded from https://academic.oup.com/gji/article/101/3/739/602971 by guest on 21 August 2022

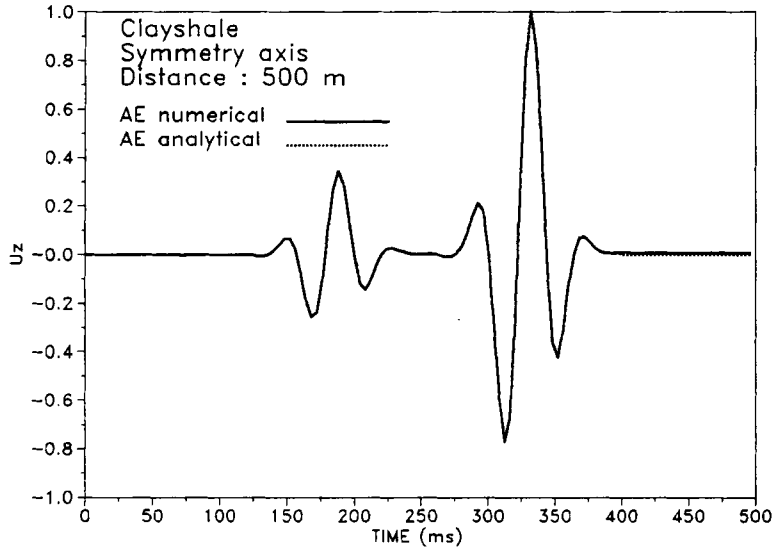

Figure 4. Time history comparison between the analytical and numerical AE solutions at the symmetry axis. Material is clayshale. The station is located at a distance of 500 m from the source.

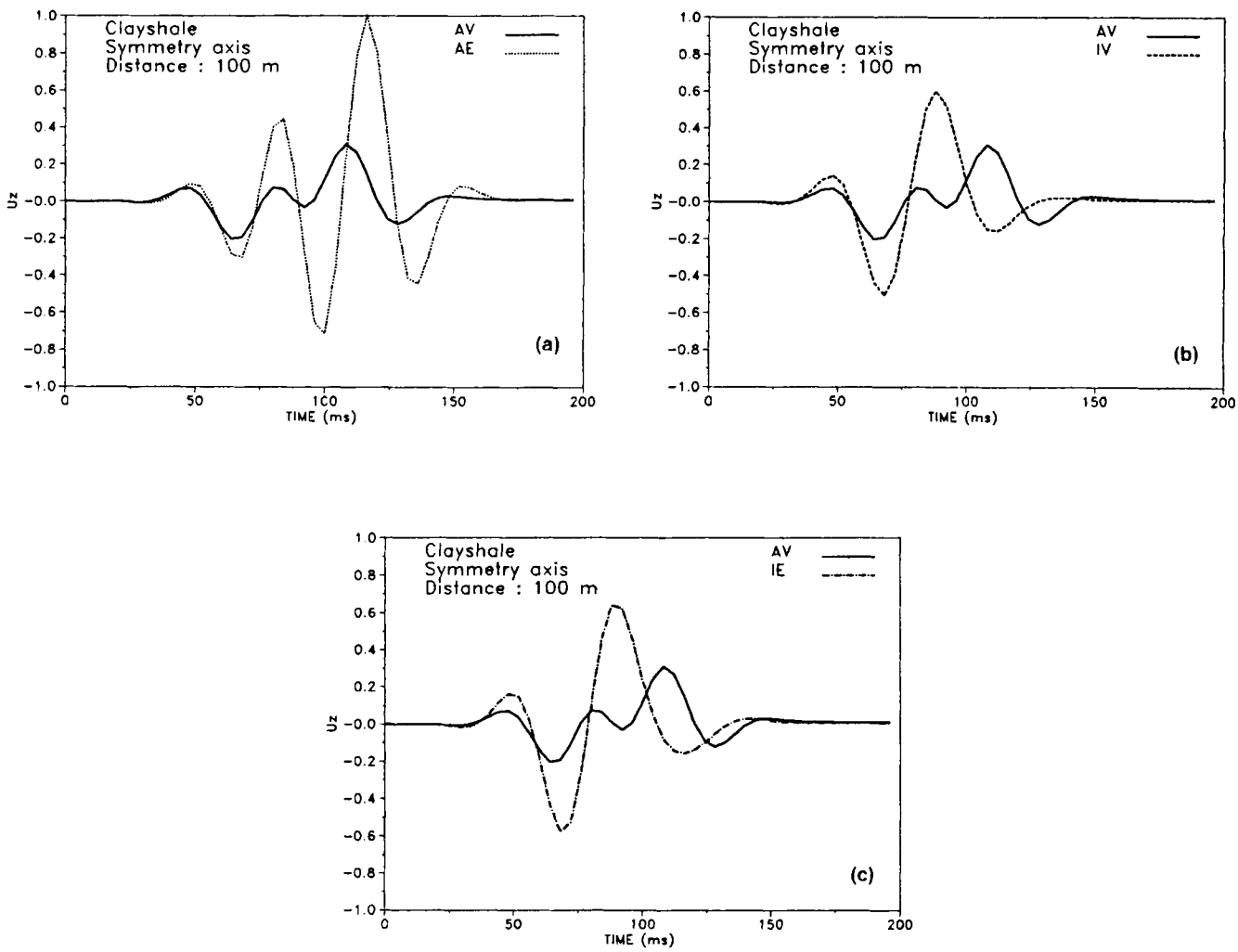

Figure 5. Time history comparison between the numerical AV rheology at the symmetry axis and: (a) AE rheology, (b) IV rheology, (c) IE rheology. Material is claysahle. The station is located at a distance of 100 m from the source.

Downloaded from https://academic.oup.com/gji/article/101/3/739/602971 by guest on 21 August 2022

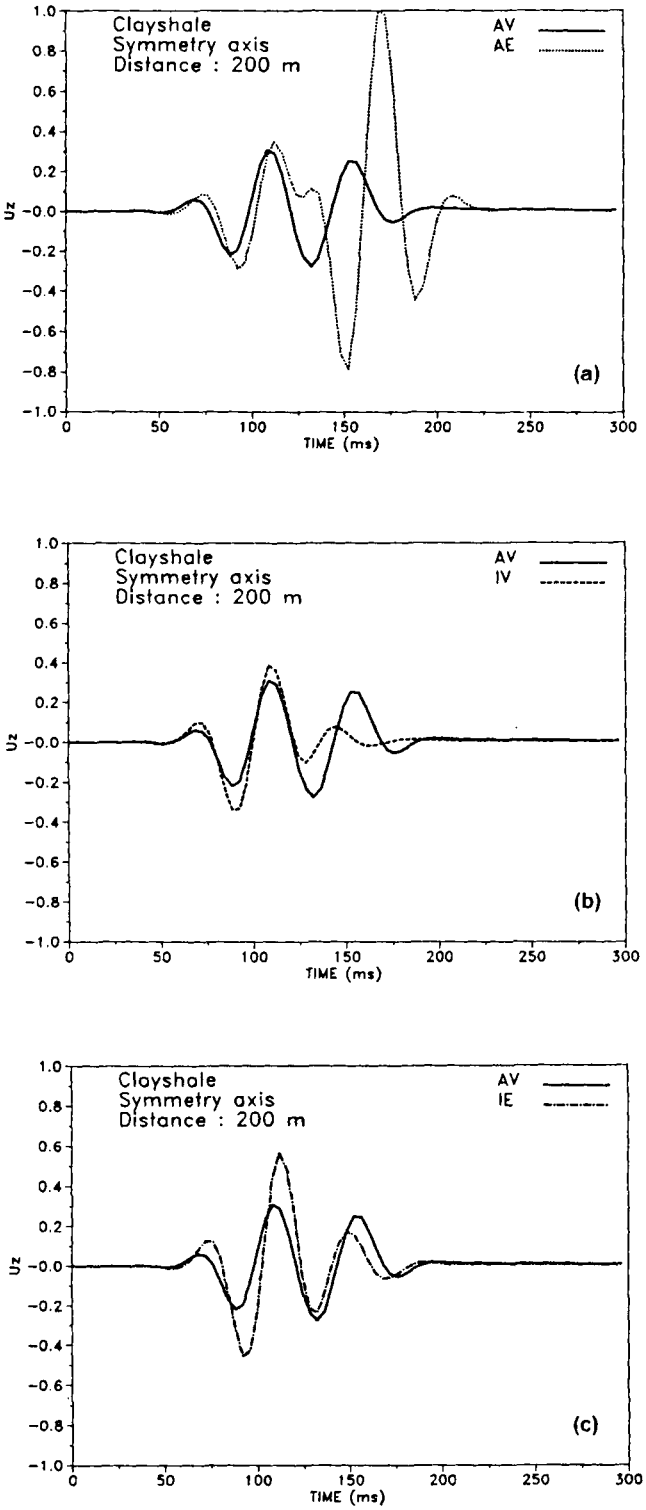

Figure 6. Time history comparison between the numerical AV rheology at the symmetry axis and (a) AE rheology, (b) IV rheology, (c) IE rheology. Material is clayshale. The station is located at a distance of 200 m from the source.

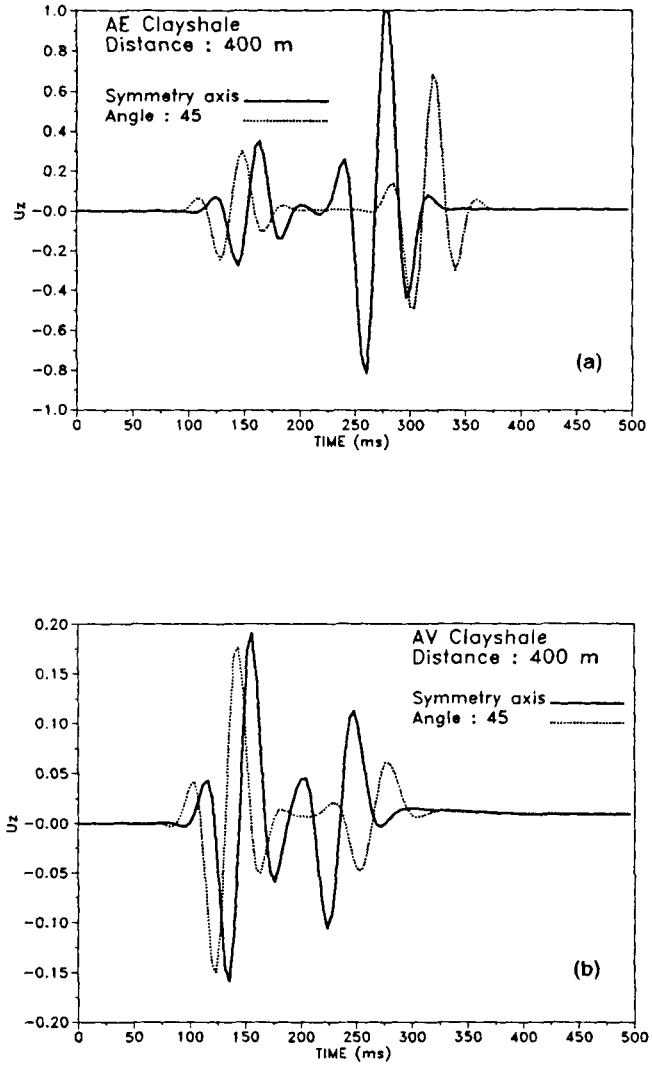

Figure 7. Time history comparison between two stations located at a distance of 400 m from the source, in the symmetry axis and at $\theta = \pi/4$, respectively, (a) AE rheology, (b) AV rheology. Material is clayshale.

The problem of implementing Boltzmann's superposition principle in the equation of motion is solved by assuming frequency-domain rational kernels. In this way the time-domain equation of motion can be written in differential form by introducing additional variables in the formulation. The examples show wave propagation in 2-D transversely isotropic–viscoelastic clayshale and sandstone compared with the isotropic and elastic rheologies. The simulations show the characteristics predicted by the theory, i.e., anisotropic attenuation and velocity dispersion, and important differences in waveform, amplitude and arrival time compared to the more simple rheologies.

The simulation theory presented in this paper could be the basis for developing realistic forward modelling codes; for instance, reflection and refraction surveys, vertical seismic profile, well to well propagation, etc. Another potential application is in earthquake modelling where anelastic and anisotropic effects can be expected to play a significant role if low Q anisotropic layers are present.

ACKNOWLEDGMENTS

The author wishes to thank the Alexander von Humboldt Foundation which enabled him to carry out this work at

Downloaded from https://academic.oup.com/gji/article/101/3/739/602971 by guest on 21 August 2022

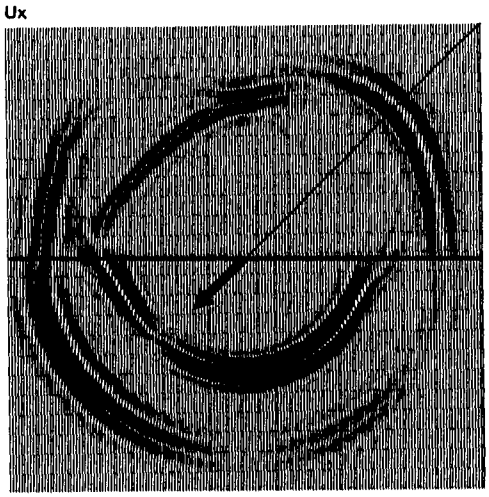

(a)

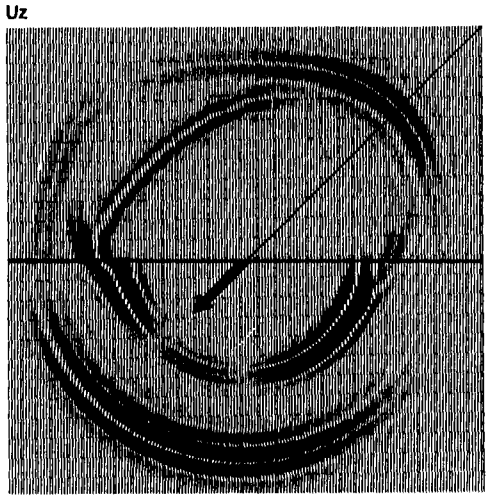

(b)

Figure 8. Snapshots at $t = 0.32$ s for an inhomogeneous medium composed of TIV sandstone (upper half-space) and IE sandstone (lower half-space), (a) u_x component, (b) u_z component. The sandstone symmetry axis and the directional force make an angle $\beta = \pi/4$ with the vertical axis. The source time history is given by equation (31).

Hamburg University. Thanks to Dr D. Kosloff and Professor A. Behle for fruitful discussions, and to the reviewers for helpful comments on the manuscript. Part of this work was supported by project EOS (Exploration Oriented Seismic Modelling and Inversion), part of Section 3.1.1.B of Joule Research and Development Programme of the Commission of the European Communities.

REFERENCES

Alekseev, A. S. & Mikhailenko, B. G., 1980. The solution of dynamics problems of elastic wave propagation in inhomogeneous media by a combination of partial separation of variables and finite difference methods, *J. Geophys.*, **48**, 161–172.

Biot, M. A., 1962. Generalized theory of acoustic propagation in porous dissipative media, *J. Acoust. Soc. Am.*, **34**, 1254–1264.

Booth, D. C. & Crampin, S., 1983. The anisotropic reflectivity technique: theory, *Geophys. J. R. astr. Soc.*, **72**, 755–766.

Borcherdt, R. D. & Wennerberg, L., 1985, General *P*, type-*I S*, and type-*II S* waves in anelastic solids; inhomogeneous wavefields in low-loss solids, *Bull. seism. Soc. Am.*, **75**, 1729–1763.

Buchen, P. W., 1971. Plane waves in linear viscoelastic media, *Geophys. J. R. astr. Soc.*, **23**, 531–542.

Carcione, J. M., Kosloff, D. & Kosloff, R., 1988a. Wave propagation simulation in a linear viscoacoustic medium, *Geophys. J. R. astr. Soc.*, **93**, 393–407.

Carcione, J. M., Kosloff, D. & Kosloff, R., 1988b. Viscoacoustic wave propagation simulation in the earth, *Geophysics*, **53**, 769–777.

Carcione, J. M., Kosloff, D. & Kosloff, R., 1988c. Wave propagation simulation in a linear viscoelastic medium, *Geophys. J. R. astr. Soc.*, **95**, 597–611.

Carcione, J. M., Kosloff, D. & Kosloff, R., 1988d. Wave propagation simulation in an anisotropic (transversely isotropic) medium, *Q. J. Mech. Appl. Math.*, **41**, 319–345.

Christensen, R. M., 1982. *Theory of Viscoelasticity, an Introduction*, Academic Press, New York.

Crampin, S., 1985. Evaluation of anisotropy by shear-wave splitting, *Geophysics*, **50**, 142–152.

Day, S. M. & Minster, J. B., 1984. Numerical simulation of attenuated wavefields using a Pade approximant method, *Geophys. J. R. astr. Soc.*, **78**, 105–118.

Emmerich, H. & Korn, M., 1987. Incorporation of attenuation into time-domain computations of seismic wave fields, *Geophysics*, **52**, 1252–1264.

Fryer, G. J. & Frazer, N., 1987. Seismic waves in stratified anisotropic media—II. Elastodynamic eigensolutions for some anisotropic solids, *Geophys. J. R. astr. Soc.*, **91**, 73–101.

Gajewski, D. & Pšenčík, I., 1988. Ray synthetic seismograms for a 3-D anisotropic lithospheric structure, *Phys. Earth planet. Inter.*, **51**, 1–23.

Geertsma, J. & Smit, D. C., 1961. Some aspects of elastic wave propagation in fluid-saturated porous solids, *Geophysics*, **26**, 169–181.

Hamilton, E. L., Buchen, H. P., Keir, D. L. & Whitney, J. A., 1970. Velocities of compressional and shear waves in marine sediments determined in situ and from a research submarine, *J. geophys. Res.*, **75**, 4039–4049.

Jones, T. D., 1986. Pore fluids and frequency-dependent wave propagation in rocks, *Geophysics*, **51**, 1939–1953.

Kosloff, D. & Baysal, E., 1982. Forward modeling by a Fourier method, *Geophysics*, **47**, 1402–1412.

Kosloff, D., Reshef, M. & Loewenthal, D., 1984. Elastic waves calculations by the Fourier method, *Bull. seism. Soc. Am.*, **74**, 875–891.

Krebes, E. S. & Hron, F., 1980. Ray-synthetic seismograms for *SH*-waves in anelastic media, *Bull. seism. Soc. Am.*, **70**, 29–46.

Kummer, B., Behle, A. & Dorau, F., 1987. Hybrid modeling of elastic-wave propagation in two-dimensional laterally inhomogeneous media, *Geophysics*, **52**, 765–771.

Lamb, J. & Richter, J., 1966. Anisotropic acoustic attenuation with new measurements for quartz at room temperatures, *Proc. R. Soc. Lond.*, **A293**, 479–492.

Martynov, V. N. & Mikhailenko, B. G., 1984. Numerical modelling of propagation of elastic waves in anisotropic inhomogeneous media for the half-space and the sphere, *Geophys. J. R. astr. Soc.*, **76**, 53–63.

Mc Donal, F. J., Angona, F. A., Mills, R. L., Sengbush, R. L., Van Nostrand, R. G. & White, J. E., 1958. Attenuation of shear and compressional waves in Pierre shale, *Geophysics*, **23**, 421–439.

Downloaded from https://academic.oup.com/gji/article/101/3/739/602971 by guest on 21 August 2022

Mikhailenko, B. G., 1985. Numerical experiments in seismic investigations, *J. Geophys.*, **58**, 101–124.

Murphy, W. F., Winkler, K. W. & Kleinberg, R. L., 1986. Acoustic relaxation in sedimentary rocks: Dependence on grain contacts and fluid saturation, *Geophysics*, **51**, 757–766.

O'Connell, R. J. & Budiansky, B., 1977. Viscoelastic properties of fluid-saturated cracked solids, *J. geophys. Res.*, **82**, 5719–5735.

Szilard, J., 1982. *Ultrasonic Testing, Non-Conventional Testing Techniques*, John Wiley & Sons, New York.

Tal-Ezer, H., Carcione, J. M. & Kosloff, D., 1989. An accurate and efficient scheme for wave propagation in linear viscoelastic media, *Geophysics*, submitted.

Virieux, J., 1986. *P–SV* wave propagation in heterogeneous media: velocity–stress finite-difference method, *Geophysics*, **51**, 889–901.

White, J. E., 1982. Computed waveforms in transversely isotropic media, *Geophysics*, **47**, 771–883.

Downloaded from https://academic.oup.com/gji/article/101/3/739/602971 by guest on 21 August 2022